

Application of high-frequency Granger causality to analysis of epileptic seizures and surgical decision making

*Charles M. Epstein, †Bhim M. Adhikari, *‡§Robert Gross, ‡Jon Willie, and †¶Mukesh Dhamala

Epilepsia, **(*) :1–10, 2014
doi: 10.1111/epi.12831

SUMMARY

Objective: In recent decades intracranial EEG (iEEG) recordings using increasing numbers of electrodes, higher sampling rates, and a variety of visual and quantitative analyses have indicated the presence of widespread, high frequency ictal and preictal oscillations (HFOs) associated with regions of seizure onset. Seizure freedom has been correlated with removal of brain regions generating pathologic HFOs. However, quantitative analysis of preictal HFOs has seldom been applied to the clinical problem of planning the surgical resection. We performed Granger causality (GC) analysis of iEEG recordings to analyze features of preictal seizure networks and to aid in surgical decision making.

Methods: Ten retrospective and two prospective patients were chosen on the basis of individually stereotyped seizure patterns by visual criteria. Prospective patients were selected, additionally, for failure of those criteria to resolve apparent multilobar ictal onsets. iEEG was recorded at 500 or 1,000 Hz, using up to 128 surface and depth electrodes. Preictal and early ictal GC from individual electrodes was characterized by the strength of causal outflow, spatial distribution, and hierarchical causal relationships.

Results: In all patients we found significant, widespread preictal GC network activity at peak frequencies from 80 to 250 Hz, beginning 2–42 s before visible electrographic onset. In the two prospective patients, GC source/sink comparisons supported the exclusion of early ictal regions that were not the dominant causal sources, and contributed to planning of more limited surgical resections. Both patients have a class I outcome at 1 year.

Significance: GC analysis of iEEG has the potential to increase understanding of preictal network activity, and to help improve surgical outcomes in cases of otherwise ambiguous iEEG onset.

KEY WORDS: High frequency oscillations, Network analysis, Seizure localization, Epilepsy surgery.



Dr. Charles M. Epstein is Professor of Neurology at Emory University School of Medicine.

Of 2.5 million people with epilepsy in the United States¹ and at least 40 million worldwide,² 30–40% have seizures that are refractory to medication,^{3,4} making them potential

candidates for epilepsy surgery.⁵ Up to 40% of patients who undergo presurgical evaluation have seizures that are not adequately localized by noninvasive testing.³ Yet a large fraction of those who undergo intracranial EEG (iEEG) for an apparently nonlesional focus never progress to surgical resection,⁶ and surgery leads to long-term remission in only around 40–60% of cases.^{6,7} There are no universally established electrophysiologic criteria to identify the seizure-onset zone.⁸ Larger numbers of electrodes implanted in recent years have not necessarily produced greater clarity in localization.^{9,10} Patients who have undergone extensive invasive procedures may fail to receive curative surgery because of the limited ability to resolve complex iEEG patterns.

Accepted September 8, 2014.

*Department of Neurology, Emory University School of Medicine, Atlanta, Georgia, U.S.A.; †Department of Physics and Astronomy, Georgia State University, Atlanta, Georgia, U.S.A.; ‡Department of Neurosurgery, Emory University School of Medicine, Atlanta, Georgia, U.S.A.; §Coulter Department of Biomedical Engineering, Georgia Institute of Technology, Atlanta, Georgia, U.S.A.; and ¶Neuroscience Institute, Center for Behavioral Neuroscience, Georgia State and Georgia Tech Center for Advanced Brain Imaging, Atlanta, Georgia, U.S.A.

Address correspondence to Charles M. Epstein, Department of Neurology, 1365A Clifton Road, NE, Atlanta, GA 30322 U.S.A. E-mail: charles.epstein@emory.edu

Wiley Periodicals, Inc.

© 2014 International League Against Epilepsy

Recent innovations in ictal analysis such as infra-slow activity and high-frequency oscillations (HFOs) have extended classic visual identification of the seizure-onset zone,^{8,11–15} often using commercially available macro-electrodes.¹⁶ Visually defined ictal HFOs have shown promise in narrowing the boundaries of surgical resections.¹⁴ At present, terminology for the various fast activities is not entirely consistent, and all will be referred to simply as ictal HFOs.⁸ A large number of mathematical techniques including coherence,¹⁷ partial directed coherence,¹⁸ time-frequency analysis,^{19,20} nonlinear dynamics,^{21,22} and the directed transfer function^{23–25} have also been proposed for analyzing the network characteristics of ictal and interictal activity. However, few of these methods have been applied to HFO activity, or to the specific problem of resolving seizure onsets when iEEG criteria are ambiguous. Methods based on autoregression or coherence cannot provide unambiguous information about direction and patterns of information spread.²³ And, especially at high frequencies, both visual and quantitative analysis may be biased by small differences in electrode location relative to ictal networks, which affect the relative amplitude and even the frequency of recorded iEEG activity.

Granger causality (GC) is a statistical technique used to determine whether one time series is useful in forecasting another. If such prediction is successful, the first, predicting time series, is said to be causal to the second. There have been few prior reports of GC analysis applied to iEEG. In an animal model of temporal lobe epilepsy, distinct patterns of directional GC relationships were found within rat hippocampi bilaterally, prior to and during seizure onset.²⁶ Franaszczuk et al.¹⁹ applied the related directed transfer function to mesial temporal seizures in three human patients, and reported that it could accurately determine patterns of seizure onset and propagation, including patterns of flow that are not readily apparent from visual inspection. These analyses appear to have involved conventional EEG frequencies of 70 Hz and below. To our knowledge, GC and related techniques have not been applied to the clinical problem of identifying the seizure onset zone, at frequencies including HFOs, in cases where inception appears to be ambiguous or near-simultaneous in widely separated regions of the brain.

We describe here our initial results in analyzing iEEG seizure onsets using GC, and then in applying GC prospectively to assist surgical decision making in two cases following iEEG. Organized seizure-related activity detected prior to any visible ictal discharge will be described provisionally as “preictal.” Throughout this article, we hypothesize that electrode sites that sample relative causal sources are in fact driving electrode sites that reflect relative causal sinks, and that the former are more likely to represent crucial nodes of a widespread ictal network.

METHODS

Patient selection

GC analysis was performed retrospectively in 10 patients and prospectively in 2. iEEG was recorded from adult patients who had undergone electrode implantation using combinations of depth electrodes, subdural strips, and grids. Specific retrospective patients were chosen for analysis from the epilepsy monitoring unit list when their electrographic seizures appeared to have a stereotyped pattern of onset and propagation. Visual criteria for ictal onset included appearance at classic EEG frequencies, initial frequency of the ictal discharge, background suppression, infraslow DC shifts, and ictal HFOs. No attempt was made to include every iEEG patient, or every seizure from every patient, because of the intensive processing required. These studies were approved by the Emory University School of Medicine Institutional Review Board.

In the prospective portion of the study, patients were chosen based on the condition of stereotyped but ambiguous visual onset, that is, ictal iEEG activity was consistent across multiple seizures, but visual criteria for iEEG seizure onset were inadequate or contradictory. Additional information was considered important for surgical decision making when a single definitive site of resection could not be selected on the basis of iEEG augmented by combinations of clinical semiology, 3T anatomic magnetic resonance imaging (MRI), positron emission tomography (PET), single photon emission computed tomography (SPECT), magnetoencephalography (MEG), neuropsychological assessment, and/or functional MRI (fMRI) mapping.

iEEG recording

Patients in this study underwent implantation of depth electrodes, subdural grids, and/or strip electrodes (Ad-Tech Medical, Racine, WI, U.S.A.) in various combinations according to the individual presurgical localization hypothesis. Recordings were made with an XLTEK system (Natus Medical, San Carlos, CA, U.S.A.) using up to 128 electrodes. Initial oversampling and a hardware anti-aliasing filter were followed by linear phase finite impulse response (FIR) filters with an order of 30, set to just below the Nyquist frequency for the final sampling rate of 500 or 1,000 Hz.

Granger causality analysis

Digitized iEEG time series data underwent spectral analysis for power, coherence, and Granger causality spectra.²⁷ Power reflects the level of synchrony among the neuronal systems within a recording electrode, coherence reflects inter-recording synchrony, and Granger causality reflects a causal influence from one recording to another. We computed GC spectra and net causal outflow spectra in sliding time windows of length 0.5 s, which included 250 time points for the data recorded at 500 Hz and 500 time-points for the data recorded at 1,000 Hz. We chose the

sliding window size from various window sizes between 0.2 and 1 s based on the optimal trade-off between spectral resolution and smoothing. The GC and power spectra had a frequency resolution of 1 Hz, and we focused on the activity in the frequency range from 50 Hz to the Nyquist frequency (half of the sampling rates, 500 Hz or 1,000 Hz). We used Geweke formulation of spectral causality,²⁸ applying parametric and nonparametric estimation approaches.^{27,29} The difficulty of finding an optimal model order in the parametric approach was circumvented by comparing power spectra from the nonparametric and parametric approaches at different model orders and choosing the model order yielding the lowest power difference. Time-varying power was computed by using complex-Morlet prototype-based continuous wavelet transforms.^{27,29} GC spectra and net causal outflow spectra were computed in sliding time windows of length 0.5 s, which included 250 time points for the data recorded at 500 Hz and 500 time points for the data recorded at 1,000 Hz. The frequency resolution in all of these calculations was 1 Hz. The multichannel time series data ranged in length from 6 s to 60 s. Net outflows were calculated by the difference between total outflow to all electrodes from a given electrode and total inflow to the given node from all others. The net outflows were further integrated over the entire frequency range to find the time domain net outflow. We further integrated causal outflow over time range and sorted out channel-by-channel outflows according to the order of descending values, which allowed us to identify the first several channels in the descending order as the strongest causal sources. These strongest sources were then used in more limited hierarchical comparisons. Visual and GC localization of iEEG seizure onset were considered consistent if the leading visual electrodes and strongest sources were identical or lay within the resection margins.

Some of the findings in our first eight retrospective cases have been described in our previous technical report.³⁰ In the very earliest patients, GC samples lasting several seconds were taken from 2 to 10 channels that included the initial visual iEEG onset. Subsequent analysis included the entire recorded set of 40–128 electrodes, and sample duration was extended up to 60 s to capture earlier development of significant GC outflow. For eight retrospective patients, additional 30 s interictal samples were also taken at times separated by at least 1 h from known electrographic seizures, to evaluate the possible presence of significant GC interictally. The interictal samples were selected to be free, as much as possible, from artifacts and sustained interictal discharges. Channels with unavoidable artifacts were deleted. Depending on the available data, the first three preictal seconds or the entire interictal sample were used to compute time windowed GC spectra and standard deviations of GC spectra channel by channel. The choice of three standard deviations for defining the onset of significant causality was based on a general three-sigma rule of statistics that 99.73% of the values (equivalent significance $p < 0.01$) in normal

or approximately normal distribution lie within three standard deviations of the mean. The Wilcoxon rank-sum test was performed on maximum GC values from the interictal and immediately preictal sample intervals, to compute the possibility that the occurrence of GC outflow in the preictal timespan was a random event.

Illustrating the extensive spatial relationships among GC sources and visible iEEG is challenging, so their complexity will be unfolded gradually in successive figures.

RESULTS

Findings in retrospective cases

Figure 1 illustrates an early result from our retrospective series. Visual analysis including conventional EEG frequencies, sustained HFOs, and DC shifts (not shown) indicated that the first recognizable ictal activity occurred at 90 Hz in a strip electrode placed over the parahippocampal gyrus, followed approximately 200 msec later by 65 Hz activity in an anterior hippocampal depth electrode. By multiple visual criteria including iEEG onset time, frequency,^{31,32} and amplitude, the parahippocampal strip electrode was thought to reflect the earliest ictal discharge, and thus to best indicate the ictal-onset zone. However, GC analysis confined to those two electrodes demonstrated that the anterior temporal depth electrode was easily the more powerful causal source. In addition, strong GC source activity was present in the anterior hippocampus during the first half-second of the iEEG sample, at a time when no ictal activity could be recognized by eye. This provocative result encouraged us to pursue further case studies and to perform more comprehensive GC analyses.

Figure 2 represents a more extensive recording from the retrospective series, but includes, for the sake of clarity, only a subset of all implanted intracranial electrodes. Significant net GC outflow appeared in discontinuous bursts beginning 32 s before visible iEEG seizure onset. The figure shows a later brief GC burst 5 s prior to that onset. The latter is characterized by DC shifts and classic ictal discharges in left temporal depth and mesial temporal strip electrodes. The GC causal network appears more widespread than the earliest ictal EEG activity, extending to portions of a left temporal grid (upper 11 channels). GC outflow and ictal activity do not appear fully congruous.

Nine of the 10 retrospective patients underwent surgery, as summarized in Table 1. For patient 2, both visual analysis and preictal GC indicated right temporal origin, but the strongest GC sources were in the superior temporal gyrus, which was spared from the resection; she relapsed briefly at 8 months. Patient 7 underwent unsuccessful stereotactic laser amygdalohippocampectomy, had a more complete anterior temporal lobectomy 3 months later, and has been in remission since. Perhaps most interesting was patient 3 (Fig. 3), who underwent left central multiple subpial transections at the electrode locations circled in the figure, but

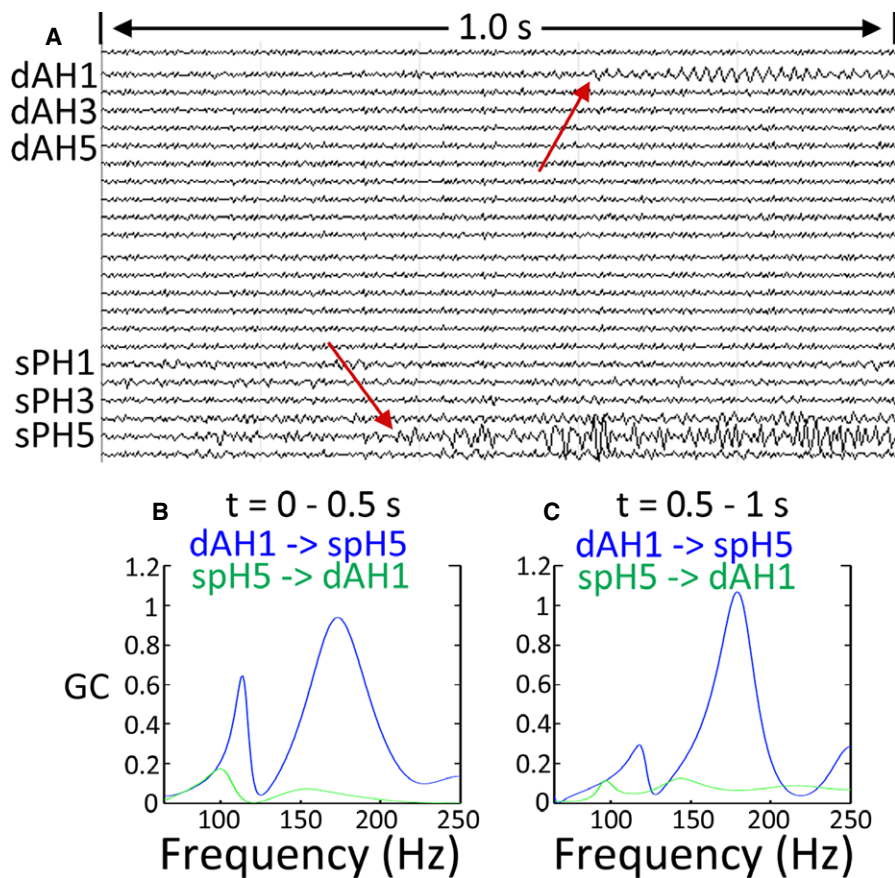


Figure 1.

(A) One-second intracranial EEG sample containing a combination of depth and strip electrodes, recording ictal onset activity from the left temporal lobe. HF = 240, LF = 40, nominal sensitivity = 20 $\mu\text{V}/\text{mm}$, sampling rate = 500 Hz. dAH1–7 are anterior hippocampal depth electrodes; sPH1–5 are strip electrodes overlying the parahippocampal gyrus. (Every other electrode is labeled for clarity.) Sustained ictal activity is seen earlier, at higher amplitude, and at higher frequency (90 Hz) in the fifth parahippocampal strip electrode (lower red arrow). Sustained ictal activity at 65 Hz appears later in the first hippocampal depth electrode (upper red arrow). (B) Granger causality (GC) analysis involving only those two electrodes shows that during the time interval 0–0.5 s, dAH1 is a strong causal source driving sPH5 at peak frequencies around 175 Hz, whereas sPH5 has very little causality in regard to dAH1. During this time no ictal activity can be recognized in the depth electrodes. Similar strong causality in the same direction is present at similar frequencies in the second half second, when ictal high frequency oscillations below 100 Hz dominate the visual record.

Epilepsia © ILAE

had no clinical improvement until major medication changes 1 year later. Retrospective GC analysis in this patient showed preictal and early ictal GC outflow most prominently in the superior parietal area, rather than the left central region identified by visual criteria.

Significant GC activity was found before visible iEEG seizure onset in all 12 retrospective and prospective patients, at frequencies from 80 Hz up to the Nyquist limit of 250 Hz. GC onset was found 2–10 s prior to iEEG onset in the first eight retrospective patients.³⁰ With the recognition that increased GC can occur in intermittent bursts, and with the collection of longer samples, significant GC activity has subsequently been recorded up to 42 s before iEEG seizure onset. In two patients, significant GC preceded the appearance of herald spikes, which have often been considered to indicate iEEG seizure onset.

In general, recording sites associated with prominent GC outflow were more widely distributed than those that were visibly involved at iEEG onset (Fig. 2), and tended to be consistent throughout the preictal interval (Fig. 3), but often were not completely congruous with the electrodes initiating visible ictal activity. Traditional visual evaluation failed to reveal this high frequency activity using any combination of gain, filter settings, and time scales.³³ Significant GC was not found in any of the remote interictal samples. The Wilcoxon test on interictal versus immediately preictal GC gave a z-statistic of 3.95 with $p = 0.00008$, thus rejecting the null hypothesis that the increased GC outflow in the immediately preictal time-span was a random event.

Using wavelet analysis, preictal HFOs associated with GC were low in amplitude, generally not exceeding 10 μV .

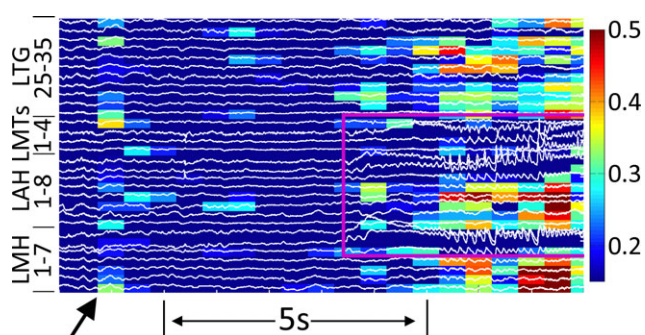


Figure 2.

GC outflow sources from 50 to 250 Hz (color scale) overlaid on a subset of iEEG channels before and during visible ictal onset. Significant GC onset began 32 s prior to visible iEEG onset. Clinical onset began 30 s after visible iEEG onset. HF = 100, LF = 0.3, nominal sensitivity = 100 $\mu\text{V}/\text{mm}$, GC outflow scale on the right. LTG, portion of a left temporal grid, LMTs, left midtemporal strip, LAH, left anterior hippocampal depths, LMH, left midhippocampal depths. Arrow: onset of significant net GC outflow. Purple outline: ictal onset. GC distribution suggests both preictal and ictal high frequency network activity. Note that both before and after iEEG seizure onset, GC outflow is more widespread than the initial visible ictal discharge.

Epilepsia © ILAE

However, as noted by others^{34,35} and shown in Figure S1, preictal HFOs could be identified across a broad spectrum of frequencies. Bursts of increased spectral power generally correspond with epochs of increased GC flow between multiple electrodes. Additional quantitative methods, graphics, and results described more thoroughly in the companion paper include wavelet power, coherence, total interdependence, and spectral and temporal Granger causality.³⁰

Prospective cases

Prospective case 1 was a 32-year-old left-handed man with medically refractory focal seizures and secondary generalization of 3 years duration. MRI showed right

hippocampal sclerosis plus Dandy-Walker malformation, hypoplastic cerebellum, and numerous areas of heterotopic gray matter that were particularly prominent in the right posterior occipital and parietal regions. iEEG recorded eight clinically and electrographically stereotyped seizures with earliest visible iEEG onset in the form of fast narrow spikes and beta activity from a single right occipital grid electrode, ROg61, which was otherwise remote from later-appearing ictal discharges in the temporal lobe (Fig. 4A). In this case, we used GC to test a simple binary hypothesis concerning electrode ROg61: that it was either a causal source or sink in relation to the temporal lobe electrodes (Fig. 4B–C). The GC result (Fig. 4D) indicated that ROg61 was in fact a causal sink despite its earlier visual iEEG onset. Based in part on this result, we chose to ignore the early discharge in ROg61 (along with the extensive anatomic abnormalities in the right parietal and occipital lobes) and perform a standard right temporal lobectomy. The patient remains seizure-free and back at work 1 year later.

Prospective case 2 was a 35-year-old left-handed man with focal seizures and rare generalization following reported *Haemophilus influenzae* meningitis in infancy. 3T anatomic MRI showed atrophy of the right mammillary body and fornix, with no hippocampal abnormality. PET scan showed bilaterally symmetric hypometabolism in the mesial temporal lobes. Scalp video-EEG suggested onset predominantly from the right parietal-temporooccipital region, with widespread interictal epileptiform discharges in the right hemisphere. iEEG recording was made from multiple strip, grid, and amygdalohippocampal depth electrodes. Figure 5 shows a subset of all implanted intracranial electrodes, combining many of those suspected to represent ictal onset, together with preictal GC activity. Based on visual criteria, stereotyped electrographic seizures were thought to possibly begin in the top 10 strip electrodes, which extended suboccipitally. GC analysis of all iEEG electrodes showed that preictal GC network activity was widespread across the right temporal, occipital, and parietal

Table 1. Surgical outcomes in retrospective patients^a

Patient	Surgery	Initial response	Current status	Consistent GC and visual EEG
1	Anterior temporal lobectomy	SF 3 years	Same	Yes
2	Anterior temporal lobectomy	Improved	SF 3 years ^b	Partial
3	Multiple subpial transection centrally	No benefit	SF 2.5 years ^b	No
4	Selective amygdalohippocampectomy	SF 2 years	Same	Yes
5	Anterior temporal lobectomy	Improved	Improved 3 years	Yes
6	Selective amygdalohippocampectomy	SF 2 years	Same	Yes
7	Stereotactic laser ablation of hippocampus	No benefit	SF 2 years ^c	Yes
8	Anterior temporal lobectomy	Improved	SF 2 years ^b	Yes
9	Anterior temporal lobectomy	SF 1 years	Unknown ^d	Yes

SF, seizure-free.

^aOne retrospective patient declined surgery.

^bSeizure-free following medication change.

^cSeizure-free following subsequent conventional anterior temporal lobectomy.

^dLost to follow-up after 1 year.

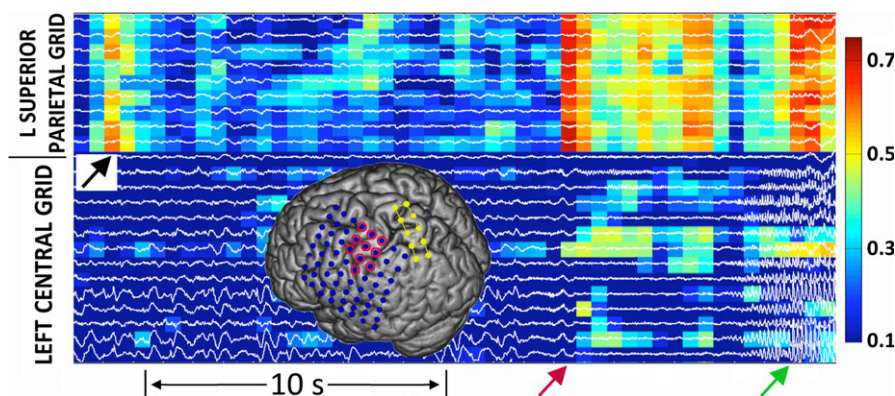


Figure 3.

Selected channels from retrospective patient 3, with GC causal outflow sources overlaid on iEEG and the inset showing the location of the electrodes. The upper block of channels represents a 10-contact grid overlying the superior parietal lobe (yellow on inset). The lower block represents part of a 64-contact central grid overlying the left frontal-parietosuperior temporal regions (blue on inset). The electrographic seizure begins with an electrodecrement and low-voltage fast activity in the central grid. Electrodes identified with visual iEEG seizure onset are circled in red. Earliest significant net GC outflow: black arrow. Visual iEEG seizure onset: red arrow. Clinical seizure onset: green arrow. HF = 100 Hz, LF = 1 Hz, nominal sensitivity = 100 μ V/mm, GC outflow scale on the right.

Epilepsia © ILAE

lobes, first becoming significant 22 s before possible herald spikes and visible iEEG onset (Fig. 6A). A comprehensive, high-resolution display of simultaneous wavelet frequencies, 120-channel iEEG, 120-channel GC, and net causal outflow is shown in Figure S1.

This initial GC analysis did not, however, resolve the strongest network sources to a single lobe. We therefore performed a second, hierarchical comparison limited to the most prominent sources at the time GC became significant (Fig. 6B). This second comparison indicated that the strongest causal source was a depth electrode in the amygdala, followed by anterior hippocampal depth electrodes. In comparison, the suboccipital neocortical electrodes were relative GC sinks. This patient also underwent a standard right anterior temporal lobectomy, including the amygdala, hippocampus, and neocortex below the first right temporal grid electrode. He had a single atypical postoperative seizure without loss of consciousness at 24 h, and has returned to full employment. In the first 6 months since surgery he reported occasional brief auras without alteration in behavior or consciousness, which have gradually been diminishing. He remains seizure-free at 1 year.

DISCUSSION

High-frequency GC analysis suggests the presence of preictal network activity that may begin earlier and cover a more extensive area than has previously been described. At the same time, it provides a new method for exploring that network and categorizing its components. The evolution of multichannel HFOs, some appearing prior to visual electrographic onset, has been reported previously in conjunction with techniques for quantifying and displaying their spatial

distribution.^{13,34,35} The further addition of GC, as proposed here, provides a potential tool for determining which of many active preictal regions comprise the strongest causal sources and thereby, perhaps, the most essential nodes of a widespread preictal network. To our knowledge, this and our previous publication³⁰ represent the first extensive descriptions of GC analysis applied to iEEG at HFO frequencies, and the first report of its use to assist in surgical planning.

For our prospective cases, Engel outcome classification is 1A and 1B³⁶ after 1 year. In these cases, GC analysis helped us to exclude from resection network locations that were visibly prominent earlier than, or simultaneous with, the eventual site of surgery. We emphasize that GC was not used simply to refine the margins of a contiguous resection—which in practice is often determined by anatomic and functional boundaries rather than by the extent of epileptiform activity. Instead, GC assisted in choosing between possible surgical sites that were widely separated across two or more lobes, and that otherwise might have led to separate resections, uncertainty about which site to approach first, or possibly deferring beneficial surgery altogether.

Our retrospective results are at least compatible with the possible utility of high-frequency GC in surgical planning. It's noteworthy that the patient whose GC and visual localization were completely inconsistent (Fig. 3) was one of the two not to benefit from the initial operation. However, the information to be gleaned from such randomly selected cases is likely to be limited. In the future we plan to confine retrospective analysis to better-defined populations.

We are aware of a potential irony in the prospective cases. With a far smaller number of iEEG electrodes, the

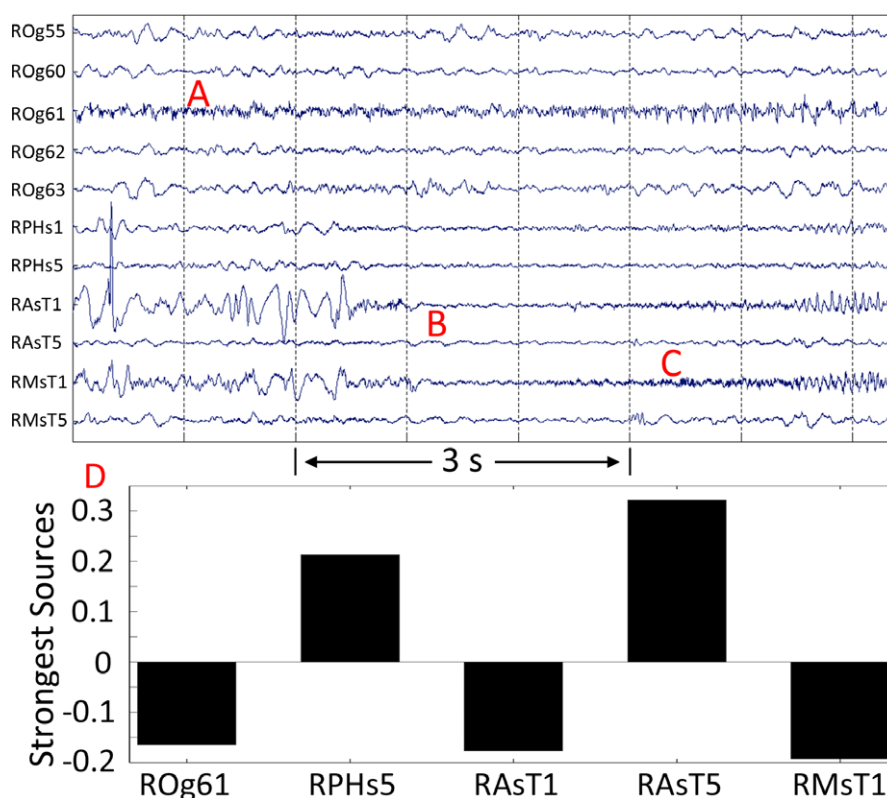


Figure 4.

Visible iEEG onset in the first prospective patient, beginning 11 s after significant GC outflow. Clinical onset began 37 s after visible iEEG onset. HF = 240, LF = 1, nominal sensitivity = 100 $\mu\text{V}/\text{mm}$. ROg, portions of a right occipital grid, RPHs, right parahippocampal strip, RAsT, right anterior subtemporal strip, RMsT, right midtemporal strip. **(A)** The earliest visually apparent discharge consists of fast activity and narrow spikes at right occipital grid electrode ROg61, preceding ictal activity in the right temporal lobe. **(B)** Electrodecrement in parahippocampal and anterior-mesial temporal strips. **(C)** High frequency oscillations progressing to ictal beta in anterior and midtemporal strip electrodes RAsT1 and RMsT1. **(D)** GC comparison limited to the electrodes that appear most involved in the initial ictal discharge, showing ROg61 and the four strongest sources in the iEEG sample. Despite being visible earliest and at high frequency, ROg61 is a causal sink over the selected time interval, whereas the strongest causal sources are the fifth, rather than the first, anterior and midtemporal strip electrodes. This finding was interpreted as evidence against ROg61 representing the ictal-onset zone or the most essential node in seizure propagation.

Epilepsia © ILAE

first visible ictal activity might have been recorded less ambiguously in the right temporal lobe prior to clinical onset, leading to the same standard resections and the same clinical outcomes. It might be argued that our sophisticated mathematics served merely to offset the increased complexity introduced by scores of additional electrodes. However, both anatomic and neurophysiologic findings suggested possible seizure onset outside the temporal lobe. We suspect that in either case, few if any modern epilepsy centers would have been content to sample iEEG only in the temporal region. Although seizure freedom during the first 6 months after surgery is a strong prognostic indicator,^{30,37–40} at present it is impossible to be certain whether the early favorable outcomes in these patients represent successful removal of the seizure-onset zone or simply interruption of major propagation pathways.

For the prospective cases, we used GC analysis in two different forms of hypothesis testing. With the first we performed a relatively simple source-sink comparison among a limited number of widely separated iEEG channels, which represented the earliest visual onsets in the occipital and temporal lobes. In similar situations, where visual criteria reduce the likely location of the seizure-onset zone to only a few electrodes, a limited GC analysis may increase confidence in the choice to ignore or include an atypical site during surgical planning. This type of comparison can be carried out with modest computational resources, provided the data have been sampled at 500 Hz or more and not tightly filtered prior to analysis. In contrast, the second prospective case required an extensive, two-stage GC comparison to identify the most prominent source among multiple channels that appeared to show multilobar onset on both GC and visual EEG evaluation. However, the small population

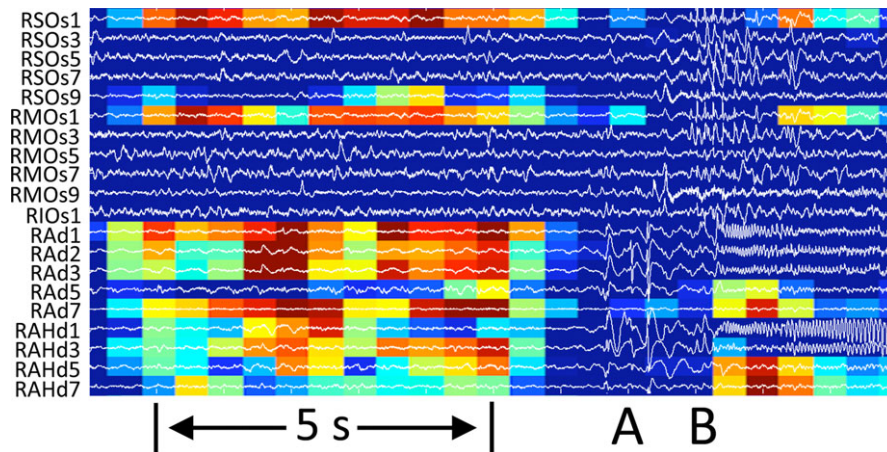


Figure 5.

GC outflow sources (color scale) overlaid on selected channels of iEEG for 12 s before and during visible ictal onset in the second prospective patient. Display parameters as in Figure 4. RSOs is a right suboccipital strip; RMOs is a midoccipital strip; RIOs1 is the most ventral electrode of an inferior occipital strip; RAd and RAHd are amygdalar and anterior hippocampal depths, respectively. A short train of spikes (**A**), more widespread than is visible in these selected channels, is followed 1-s later by a widespread polymorphic ictal discharge (**B**).

Epilepsia © ILAE

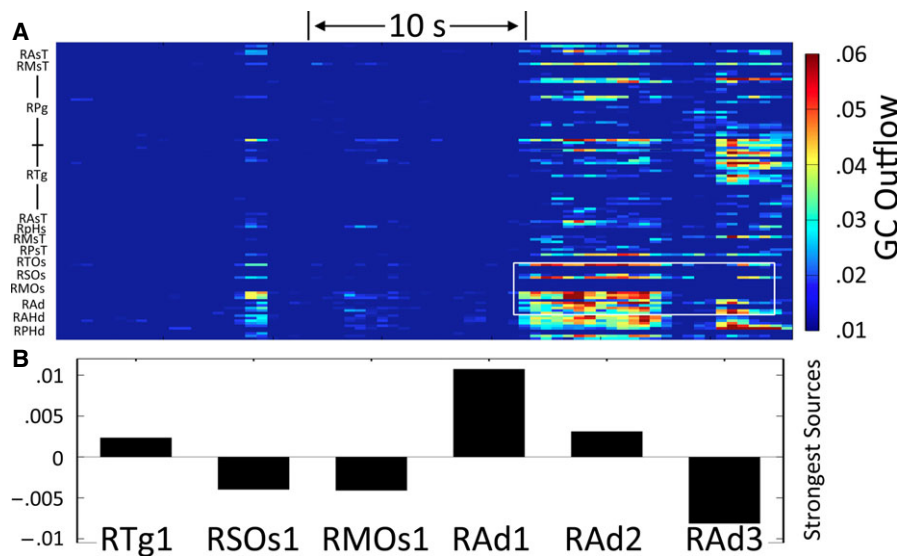


Figure 6.

(**A**) GC outflow sources for all sampled electrodes in the same patient as Figure 5, extending from 30 s prior to visible ictal onset to 4 s after. The section outlined in white at the lower right of the graph corresponds to the data selected for Figure 5. Additional electrodes: RAsT, right anterior temporal strip; RMST, right midtemporal strip; RPg, right parietal grid; RTg, right temporal grid; RPsT, right posterior temporal strip. (**B**) Pairwise GC outflow comparison limited to the six most prominent GC source electrodes, computed prior to ictal onset. The first amygdalar depth electrode is the dominant source, with the second amygdalar depth electrode next. RSOs1 and RMOs1, two sites of apparent visible early onset, are relative sinks. RTg1, a weaker relative source, was within the area of the subsequent anterior temporal resection.

Epilepsia © ILAE

of surgical cases is one of the major limitations of this study, especially in terms of improving surgical outcomes.

One technical limitation of this study is that all but the last patient were recorded at a sampling rate of 500 Hz, restricting analysis to a range below 250 Hz. This was due both to

data storage limitations and to the even longer GC processing time that is required with higher sampling rates. However, seizures recorded separately at both 500 Hz and 1,000 Hz in the last patient produced GC results that were essentially identical, both in direct comparison and after

downsampling of the seizure recorded at 1,000 Hz. As shown in Figure S1, peak frequencies of GC activity and associated wavelet power did not exceed 250 Hz. In their quantitative study of multiband ictal HFO activity, Ochi et al.³⁵ used a sampling rate of 1,000 Hz but also reported finding peak HFO frequencies no higher than 250 Hz. Further studies with wider bandwidth should help to characterize the optimum frequency range more precisely, and to investigate the relationships among the neuronal activities underlying our GC findings and the ictal/preictal HFOs previously characterized by visual and classic quantitative techniques.

The greatest impediment to GC analysis is the enormous number of calculations needed to evaluate causal relationships among large numbers of channels at high sampling rates. With a dedicated computer requiring roughly 1 h of processing for every second of data, it is challenging to complete a single ictal analysis prior to explantation of iEEG electrodes, much less evaluate the many days of interictal recording that are commonly performed on iEEG patients. The use of networked computers and steady improvements in computer speed should eventually help to alleviate this bottleneck as well. (If Moore's law continues to apply, 1 day of computer time today may be as little as 2 h in 5 years, and 15 min in a decade.) At present, our application of GC to surgical planning remains restricted to highly specific circumstances, in which (1) multiple recorded seizures are highly stereotyped on visual iEEG examination, and (2) diffuse ictal onset appears to involve multiple discontinuous sites across two or more lobes of the involved hemisphere, preventing contiguous resection. In practice, however, many days of computer time are likely to be less expensive than the hours of skilled human effort often required to classify HFOs visually, and are less dependent on human judgment.

Localizing targets for surgery in refractory epilepsy remains a complex and imperfect process, for which mathematical analysis of iEEG is unlikely to represent a panacea. At the most fundamental level, no form of data processing can identify or delineate an epileptogenic region where no electrode is present, or resolve all cases of apparent diffuse iEEG onset. However, GC is much less dependent than many other techniques on relative signal amplitude, places no restrictions on types of electrodes, and has no esoteric requirements beyond sufficient sampling rates and offline processing power. If the present results are corroborated, GC may become a useful addition to the multiplicity of techniques that contribute to increased efficacy and decreased morbidity in the surgical treatment of epilepsy.

ACKNOWLEDGMENTS

J. Andrew Ehrenberg contributed to production of the figures.

DISCLOSURE OR CONFLICT OF INTEREST

Dr. Epstein receives research funding from Medtronic. Dr. Gross receives research funding from NeuroPace, Medtronic, and Visualase, which develops products related to some of the research described in this paper; In addition, he serves as a consultant to NeuroPace, Medtronic, and Visualase. The terms of these arrangements have been reviewed and approved by Emory University in accordance with its conflict of interest policies. The remaining authors have no conflicts of interest to declare. We confirm that we have read the Journal's position on issues involved in ethical publication and affirm that this report is consistent with those guidelines.

REFERENCES

- French JA, Kanner AM, Bautista J, et al. Efficacy and tolerability of the new antiepileptic drugs II: treatment of refractory epilepsy. *Neurology* 2004;62:1261–1273.
- Litt B, Echauz J. Prediction of epileptic seizures. *Lancet Neurol* 2002;1:22–30.
- Duncan JS. Imaging in the surgical treatment of epilepsy. *Nat Rev Neurol* 2010;6:537–550.
- Kwan P, Brodie MJ. Early identification of refractory epilepsy. *N Engl J Med* 2000;342:314–319.
- Dua T, de Boer HM, Prilipko LL, et al. Epilepsy care in the world: results of an ILAE/IBE/WHO global campaign against epilepsy survey. *Epilepsia* 2006;47:1225–1231.
- Noe K, Sulc V, Wong-Kissel L, et al. Long-term outcomes after nonlesional extratemporal lobe epilepsy surgery. *JAMA Neurol* 2013;70:1003–1008.
- Dorward IG, Titus JB, Limbrick DD, et al. Extratemporal, nonlesional epilepsy in children: postsurgical clinical and neurocognitive outcomes. *J Neurosurg Pediatr* 2011;7:179–188.
- Jacobs J, Staba R, Asano E, et al. High-frequency oscillations (HFOs) in clinical epilepsy. *Prog Neurobiol* 2012;98:302–315.
- Matsuoka LK, Spencer SS. Seizure localization using subdural grid electrodes. *Epilepsia* 1993;34(Suppl. 6):8. Abstract.
- Rosenow F, Luders H. Presurgical evaluation of epilepsy. *Brain* 2001;124:1683–1700.
- Allen PJ, Fish DR, Smith SJ. Very high-frequency rhythmic activity during SEEG suppression in frontal lobe epilepsy. *Electroencephalogr Clin Neurophysiol* 1992;82:155–159.
- Fisher RS, Webber WR, Lesser RP, et al. High-frequency EEG activity at the start of seizures. *J Clin Neurophysiol* 1992;9:441–448.
- Jirsch JD, Urrestarazu E, LeVan P, et al. High-frequency oscillations during human focal seizures. *Brain* 2006;129:1593–1608.
- Modur PN, Zhang S, Vitaz TW. Ictal high-frequency oscillations in neocortical epilepsy: implications for seizure localization and surgical resection. *Epilepsia* 2011;52:1792–1801.
- Zijlmans M, Jacobs J, Kahn YU, et al. Ictal and interictal high frequency oscillations in patients with focal epilepsy. *Clin Neurophysiol* 2011;122:664–671.
- Blanco JA, Stead M, Krieger A, et al. Unsupervised classification of high-frequency oscillations in human neocortical epilepsy and control patients. *J Neurophysiol* 2010;104:2900–2912.
- Schevon CA, Weiss SA, McKhann G Jr, et al. Evidence of an inhibitory restraint of seizure activity in humans. *Nat Commun* 2012;3:1060.
- Varotto G, Tassi L, Franceschetti S, et al. Epileptogenic networks of type II focal cortical dysplasia: a stereo-EEG study. *Neuroimage* 2012;61:591–598.
- Franaszczuk PJ, Bergey GK, Durka PJ, et al. Time–frequency analysis using the matching pursuit algorithm applied to seizures originating from the mesial temporal lobe. *Electroencephalogr Clin Neurophysiol* 1998;106:513–521.
- Fujiwara H, Greiner HM, Lee KH, et al. Resection of ictal high-frequency oscillations leads to favorable surgical outcome in pediatric epilepsy. *Epilepsia* 2012;53:1607–1617.

21. Marten F, Rodrigues S, Suffczynski P, et al. Derivation and analysis of an ordinary differential equation mean-field model for studying clinically recorded epilepsy dynamics. *Phys Rev E* 2009;79:021911.
22. Blenkinsop A, Valentin A, Richardson MP, et al. The dynamic evolution of focal-onset epilepsies—combining theoretical and clinical observations. *Eur J Neurosci* 2012;36:2188–2200.
23. Franaszczuk PJ, Bergey GK, Kamiński MJ. Analysis of mesial temporal seizure onset and propagation using the directed transfer function method. *Electroencephalogr Clin Neurophysiol* 1994;91:413–427.
24. Ding L, Worrell GA, Lagerlund TD, et al. Ictal source analysis: localization and imaging of causal interactions in humans. *Neuroimage* 2007;34:575–586.
25. Wilke C, van Drongelen W, Kohrman M, et al. Neocortical seizure foci localization by means of a directed transfer function method. *Epilepsia* 2010;51:564–572.
26. Cadotte AJ, DeMarse TB, Mareci TH, et al. Granger causality relationships between local field potentials in an animal model of temporal lobe epilepsy. *J Neurosci Methods* 2010;189:121–129.
27. Dhamala M, Rangarajan G, Ding M. Analyzing information flow in brain networks with nonparametric Granger causality. *Neuroimage* 2008;41:354–362.
28. Geweke J. Measurement of linear dependence and feedback between multiple time series. *J Am Stat Assoc* 1982;77:304–313.
29. Ding M, Chen Y, Bressler S. Granger Causality: Basic theory and application to neuroscience. In Schelter B, Winterhadler M, Timmers J (Eds) *Handbook of time series analysis: recent theoretical developments and applications*. Berlin: Wiley-VCH, 2006:2437–2459.
30. Adhikari BM, Epstein CM, Dhamala M. Localizing epileptic seizure onsets with Granger causality. *Phys Rev E* 2013;88:030701(R).
31. Faught E, Kuzniecky RI, Hurst DC. Ictal EEG wave forms from epidural electrodes predictive of seizure control after temporal lobectomy. *Electroencephalogr Clin Neurophysiol* 1992;83:229–235.
32. Wetjen NM, Marsh WR, Meyer FB, et al. Intracranial electroencephalography seizure onset patterns and surgical outcomes in nonlesional extratemporal epilepsy. *J Neurosurg* 2009;110:1147–1152.
33. Schevon CA, Thompson T, Hirsch LJ, et al. Inadequacy of standard screen resolution for localization of seizures recorded from intracranial electrodes. *Epilepsia* 2004;45:1453–1458.
34. Akiyama T, Chan DW, Go CY, et al. Topographic movie of intracranial ictal high-frequency oscillations with seizure semiology: epileptic network in Jacksonian seizures. *Epilepsia* 2011;52:75–83.
35. Ochi A, Otsubo H, Donner EJ, et al. Dynamic changes of ictal high-frequency oscillations in neocortical epilepsy: using multiple band frequency analysis. *Epilepsia* 2007;48:286–296.
36. Engel J Jr, Van Ness PC, Rasmussen TB, et al. Outcome with respect to epileptic seizures. In Engel J Jr (Ed) *Surgical treatment of the epilepsies*. New York: Raven Press, 1993:609–622.
37. Bulacio JC, Jehi L, Wong C, et al. Long-term seizure outcome after resective surgery in patients evaluated with intracranial electrodes. *Epilepsia* 2012;53:1722–1730.
38. Jeha LE, Najm I, Bingaman W, et al. Surgical outcome and prognostic factors of frontal lobe epilepsy surgery. *Brain* 2007;130:574–584.
39. Jehi L, Sarkis R, Bingaman W, et al. When is a postoperative seizure equivalent to “epilepsy recurrence” after epilepsy surgery? *Epilepsia* 2010;51:994–1003.
40. Wiebe S, Blume WT, Girvin JP, et al. A randomized, controlled trial of surgery for temporal-lobe epilepsy. *N Engl J Med* 2001;345:311–318.

SUPPORTING INFORMATION

Additional Supporting Information may be found in the online version of this article:

Figure S1. Simultaneous high-resolution display of channel-averaged wavelet power, conventional visual iEEG, channelwise GC outflow, and net causal outflow in prospective case 2.